Institute of Pharmaceutical Technology[1], Goethe University, Frankfurt am Main, Germany; Nanosystem Ltd.[2], Moscow, Russia

Arylsulfatase A bound to poly(butyl cyanoacrylate) nanoparticles for enzyme replacement therapy – physicochemical evaluation

A. Mühlstein[1], S. Gelperina[2], E. Shipulo[2], O. Maksimenko[2], J. Kreuter[1]

Received October 28, 2013, accepted December 13, 2013

Dr. Jörg Kreuter, Institut für Pharmazeutische Technologie, Johann Wolfgang Goethe Universität, Max-von-Laue Str. 9, 60438 Frankfurt am Main, Germany
kreuter@em.uni-frankfurt.de

Pharmazie 69: 518–524 (2014) *doi: 10.1691/ph.2014.3250*

Arylsulfatase A (ASA) deficiency is the cause of metachromatic leucodystrophy (MLD), a lysosomal storage disease associated with severe neurological disorders. Poly(butyl cyanoacrylate) (PBCA) nanoparticles overcoated with polysorbate 80 enabled the delivery of several drugs across the blood-brain barrier to the brain suggesting that these nanoparticles also may transport ASA across this barrier. The objective of this research, therefore, was to evaluate the feasibility of loading ASA onto PBCA nanoparticles. A stable ASA-loaded PBCA nanoparticle formulation was developed that could be easily freeze-dried and stored over a period of more than 8 weeks. The maximum loading capacity for this enzyme was ~59 μg per 1 mg of PBCA. In the presence of 3 % sucrose as a lyoprotector the activity of freeze-dried ASA was found to be 100 % recoverable.

1. Introduction

Metachromatic leucodystrophy (MLD) is a fatal lysosomal storage disease which is directly caused by a deficiency of the enzyme arylsulfatase A (ASA). ASA catalyses the intralysosomal desulfation of 3-*O*-sulfogalactosylceramide (sulfatide) to galactosylceramide (von Figura 2001; Kolodny 1989). A lack of ASA results in a block of sulfatide degradation resulting in a progressive intralysosomal accumulation of sulfatide. The incidence of MLD depends on geographic regions and ethnic groups (von Figura 2001). In Europe it is estimated to be 1 in 100 000 live births (Poorthuis 1999; Heim et al. 1997). The clinical manifestations of MLD are dominated by the demyelination observed in the central and peripheral nervous systems.

Deficiency of arylsulfatase B (ASB), another lysosomal hydrolase, is leading to the accumulation of dermatan sulphate and chondroitin 4-sulfate, which results in the severe lysosomal storage disorder mucopolysaccharidosis type VI (MPS VI) or Maroteaux-Lamy syndrome. ASB catalyses the glycosaminoglycan degradation with dermatan sulfate as a natural substrate. A recombinant human *N*-acetylgalactosamine-4-sulfatase (ASB) is available on the market (Naglazyme®, BioMarin Europe Ltd.) as an enzyme replacement therapy (ERT) for the treatment of MPS VI. The efficacy of ERT in the MPS VI is limited due to rapid removal of ASB from circulation and its inability to overcome the blood brain barrier (BBB). The adsorptive binding of ASB to poly(butyl cyanoacrylate) (PBCA) nanoparticles as drug delivery systems was investigated previously (Mühlstein et. al. 2013).

Depending on the pH of the surrounding media, ASA exists as an octamer at pH 5 which dissociates into dimers at neutral pH. The ASA monomer has a molecular mass of 57 to 62 kDa depending on dregree of glycosylation and a pI of 4.3 to 4.5 (Agogbua and Wynn 1976; Gibson et al. 1987; Lukatela et al. 1998; Sommerlade et al. 1994). In contrast to ASA, ASB is a monomer with a molecular weight of around 57 kDa. Both arylsulfatases are homologous enzymes that consist of a single 500 amino acid polypeptide chain folded to a similar hatlike tertiary structure with a base of 45 Å × 70 Å and 50 Å height (Lukatela et al. 1998; Ghosh 2007). The analogy of the amino acids is about 29% (Yaghootfam et al. 2003). Differences appear in the metal ion that is present in the active site, where ASA has a Mg^{2+} and ASB Ca^{2+} (Bond et al. 1997; Lukatela et al. 1998). The metal ion is proposed to stabilize the sulfate ester during the desulfation of the substrate (Bond et al. 1997).

Due to their high molecular mass and hydrophilicity, exogenous ASA and ASB are not able to permeate across the BBB and, therefore, an effective enzyme replacement therapy of MLD is not available at present (Beck 2010; i Dali et al. 2009; Gieselmann and Krageloh-Mann 2010). The BBB is formed by endothelial cells connected by tight junctions which restricts the transport of most substances across this barrier thus enabling a well-controlled homeostasis within the brain. However, this barrier also abolishes the accessibility of most therapeutic substances including ASA and ASB to the brain and obstructs treatment of many diseases of the central nervous system (CNS) (Pardridge 2005). In general, transport over the BBB is limited to lipophilic, small molecules with a molecular mass of less than 500 Da (Rubin et al. 1999; Scheld et al. 1989). Endogenous proteins like insulin, transferrin, and neuropeptides access the brain by specific receptor-mediated transport (McGonigle et al. 2006; Pardridge et al. 2005; Pardridge et al. 2007a). These peptides, however, are exceptions; other large (> 500 Da), hydrophilic substances cannot pass across the BBB and consequently will be eliminated by renal clearance or enzymatic digestion (McGonigle et al. 2006). Possibilities for therapeutic proteins to overcome the BBB are delivery by so-called "Trojan horses" such as fusion proteins or drug-loaded liposomes or nanoparticles (Kreuter et al. 2001; Wohlfart et al. 2012; Pardridge 2007b). While fusion proteins require covalent

coupling with ligands such as transferrin, protein transduction domains, or specific antibodies, nanoparticles and liposomes can be simply loaded by incorporation or adsorption.

PBCA nanoparticles enabled the transport of a variety of drugs such as loperamide, dalargin, doxorubicin, and even larger molecules such as the nerve growth factor (NGF) over the BBB (Alyautdin et al. 1997; Alyautdin et al. 1998; Kurakhmaeva et al. 2009). The mechanism for the nanoparticle uptake into the brain appears to be receptor-mediated endocytosis followed by transcytosis as evidenced by transmission electron microscopy (Zensi et al. 2009).

The objective of the present study, therefore, was to evaluate the possibility of binding ASA to PBCA nanoparticles and to additionally compare the obtained results to the previously investigated adsorption behaviour of ASB (Mühlstein et al. 2013). Additionally, in the present study freeze-drying and storage experiments were performed for ASA as well as ASB.

2. Investigations, results, and discussion

2.1. Determination of ASA and ASB loading in PBCA nanoparticles

The amount of adsorbed enzyme was determined either indirectly by SEC (Mühlstein et al. 2013) or by a specific activity assay using *p*-nitrocatechol sulphate (pNCS) as substrate (Baum et al. 1959). The nanoparticles were separated from the unbound enzyme by centrifugation. The total amount of unbound enzyme (SEC) or amount of active enzyme (pNCS) found in the supernatant was then subtracted from the initially used sulfatase amount. It appeared that both, ASA and ASB, adsorbed on the nanoparticles did not exhibit the expected activity. In fact, the activity was ~20 % lower than expected, which might be a result of the partial deactivation of these enzymes due to their interaction with the particle surface. This phenomenon was also observed for other proteins (Mollmann et al. 2006; Koutsopoulos et al. 2007). However, the enzyme activity was recovered after desorption (Section 2.2).

It is well known, that the adsorption of drugs to the nanoparticle surface may depend on a number of parameters, among them the drug concentration, composition of the media, incubation time, temperature, etc. (Kufleitner et al. 2010; Soppimath et al. 2001). As shown by Mühlstein et al. (2013) the efficiency of the ASB adsorption to the PBCA nanoparticles was most considerably influenced by the type of a stabilizer and enzyme concentration. The contribution of other parameters, such as incubation time or temperature, was only marginal.

Thus, in the case of ASB, employment of dextran 70000 as a particle stabilizer produced a considerable adsorption, whereas in the presence of poloxamer 188 the ASB adsorption to the nanoparticles was negligible. The maximal capacity of 47 µg of ASB per mg of nanoparticles was reached after one hour. The adsorption process appeared to be more dependent on the ASB concentration than on pH (Mühlstein et al. 2013). The maximal capacity of 64.5 µg ASB per 1 mg PBCA was reached at pH 6.3 at the ASB concentration of 3000 µg/ml (Fig. 1). At lower concentrations of the ASB nearly 100 % loading (pH 7.3) was achieved. The correlation of the adsorption isotherm with the Langmuir model ($R^2 > 0.97$) suggests that ASB adsorbed as a monolayer to the surface of the PBCA nanoparticles (Mühlstein et al. 2013).

To investigate the transferability of the obtained results to the homologous enzyme ASA in the present study the influence of the pH of the adsorption media was evaluated under previously defined conditions (Fig. 2) and compared to the results obtained for ASB. The properties of the ASB and ASA are compared in Table 1.

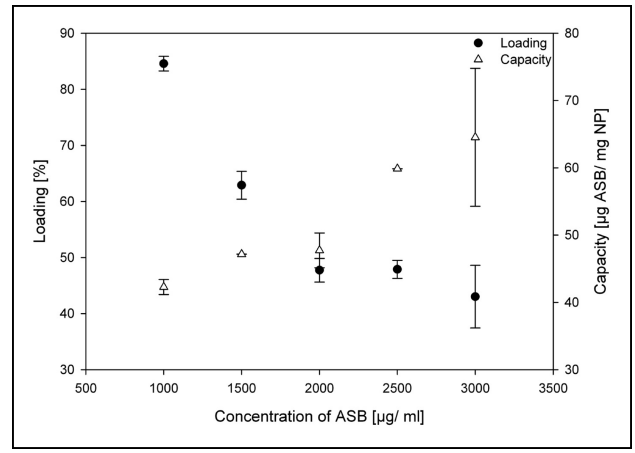

Fig. 1: Relative drug loading [%] and capacity [µg ASB/ mg PBCA] of poly(butyl cyanoacrylate) nanoparticles at different concentrations of ASB (pH 6.3, n = 3; mean ± S.D.).

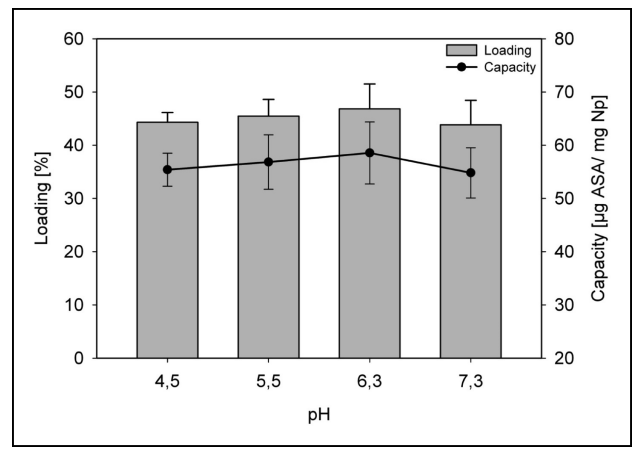

Fig. 2: Relative drug loading [%] and capacity [µg ASA/ mg PBCA] of poly(butyl cyanoacrylate) nanoparticles at different pH values of adsorption media and ASA concentration of 2500 mg/ml (n = 3; mean ± S.D.).

The results of the present study demonstrated that, similarly to ASB, there was no significant influence of pH in the range of 4.5–7.3 on the loading capacity of PBCA. The loading of ASA reached ~ 35 %, capacity was around 55 µg/mg PBCA (1246 molecules ASA/nanoparticle). Overall, there was no statistically significant difference between the efficiency of the ASA and ASB adsorption to PBCA nanoparticles (capacity) (p = 0,643).

As described earlier (Mühlstein et al. 2013), the spherical nanoparticles with a diameter of 150 nm have a surface area of 70686 nm^2, whereas the area occupied by one ASB molecule is 31.5 nm^2 (Table 1). Applying these values to Eq. (1), a maximal theoretically adsorbable amount of 120 µg ASB/mg nanoparticles was calculated (Mühlstein et al. 2013).

$$M_{\max} = \frac{MM_{ASB} \cdot C_{NP} \cdot 3}{N_A \cdot S_{ASB} \cdot d_{NP} \cdot r} \quad (1)$$

where: MM_{ASB} molecular mass of ASB (57 kDa) N_A, Avogadro constant, C_{NP}, concentration of nanoparticles (10 mg/ml), d_{NP}, density of nanoparticles (1000 mg/cm^3). r, radius of one nanoparticle (75 nm) S_{ASB}, maximal nanoparticles surface area occupied by ASB (31.5 nm^2)

Applying the same calculation method to ASA with a molecular weight of 114 kDa (dimer), an area of ~63 nm^2 occupied by an ASA dimer, and a particle diameter of 160 nm (Table 2), the maximal adsorbable amount is 113 µg/mg PBCA (2560 molecules ASA/nanoparticle). However, the adsorption experiments demonstrated that the capacity of the PBCA nanoparticles

Table 1: Properties of arylsulfatases A and B

Property	ASA	ASB
Biological function	Desulfation of 3-O-sulfogalactosylceramide (sulfatide) to galactosylceramide (Beck 2007; Gieselmann 1995)	Desulfation of dermatan sulfate and chondroitin 4-sulfate (Beck 2007; Gieselmann 1995)
Substrate	Sulfatid (Beck 2007; Gieselmann 1995)	Dermatan sulfate, chondroitin 4-sulfate (Beck 2007; Gieselmann 1995)
Disease (as a result of enzyme deficiency)	Metachromatic leucodystrophy (MLD) (Beck 2007; Gieselmann 1995)	Mucopolysaccharidosis type VI (MPS VI) (Beck 2007; Gieselmann 1995)
Isoelectric point (pI)	4.3–4.5 (Agogbua and Wynn 1976)	7.5 (Agogbua and Wynn 1976)
Configuration	Dimer at pH 7 Octamer at pH 5 (Lukatela et al. 1998)	Monomer (Lukatela et al. 1998)
MW	Depending on glycosylation 57–61 kDa (monomer) (Sommerlade et al. 1994)	ca. 57 kDa (Gibson et al. 1987)
Shape and dimensions	Hat-shaped with a base of 70 x 45 $Å^2$ and a height of 50 Å (Lukatela et al. 1998) (monomer)	
Number of amino acid residues	~ 500 (monomer), homology 29% (Yaghootfam et al. 2003)	
Metal-binding site	Mg^{2+} (Lukatela et al. 1998)	Ca^{2+} (Lukatela et al. 1998)

Table 2: Physicochemical parameters of unmodified PBCA nanoparticles, freshly prepared suspension (in MilliQ, n = 3; mean ± S.D.)

Particle size (nm)	160 ± 2
Polydispersity index (0–1.0)	0.231 ± 0,004
Zeta potential (mV)	−5.0 ± 6.5
Particle yield (%)	66.1 %

at pH 6.3 and enzyme concentration of 2.5 mg/ml only was 59.0 ± 6.0 μg/mg polymer for ASA and 60.0 ± 2.0 μg/mg polymer for ASB. This calculation of the theoretically feasible adsorption efficacy is based on the ideal adsorption conditions such as spherical particle shape, narrow polydispersity, and preserved arylsulfatase activity. However, both arylsulfatases are large proteins of above 57 kDa; hence due to steric hindrance and/or electrostatic interaction, the enzyme layer on the particle surface most probably is irregular. In the case of the ASA steric hindrance is probably even more pronounced due to its tendency for dimer formation. As a result, the effectively adsorbed enzyme amount might be lower than the theoretical value, and the adsorption does not entirely appear to follow the theoretical Langmuir adsorption pattern, which also applies to the differences between calculated maximal loading and experimental results. The regularity in distribution, on the other hand, is an indication that still processes similar to Langmuir kinetics are involved, although hydration water, Brownian mobility, and steric factors appear to prevent a closer packing of the enzyme molecules (Mühlstein et al. 2013).

The PCS measurements of the PBCA nanoparticles coated with ASA showed that variation of pH did not significantly influence the size and polydispersity (Fig. 3). The slight decrease of the particle size observed for the ASA-coated nanoparticles may be explained by reduction of the hydration shell by adsorbing enzyme (Cha et al. 2008; Krishnan et al. 2006). As shown in Fig. 4, the zeta-potential decreased slightly with adsorption of

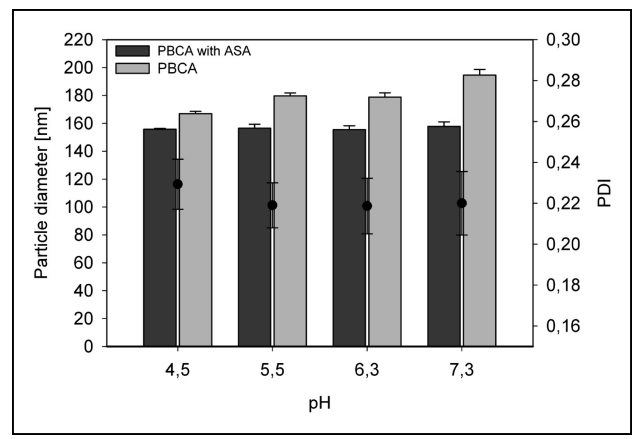

Fig. 3: Particle diameter (bars) and polydispersity index (PDI) (dots) of ASA loaded and unloaded PBCA nanoparticles at variation of media pH (n = 3, mean ± S.D.) measured with PCS.

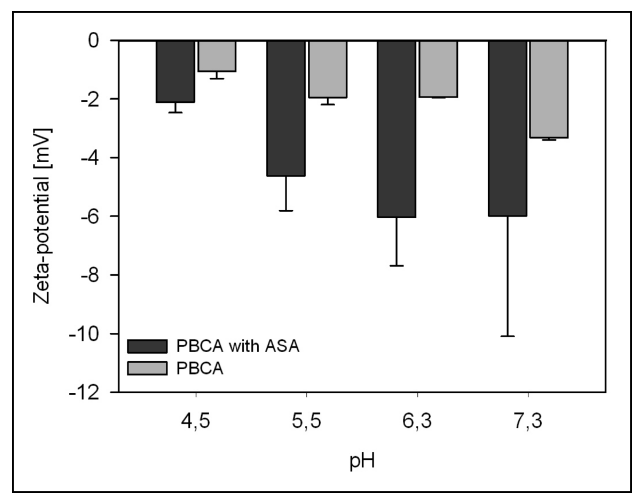

Fig. 4: Zeta-potential of ASA-loaded and unloaded PBCA nanoparticles at different pH (n = 3, mean ± S.D.) measured with PCS.

ASA, which might be due to the negative charge of ASA (pI 4.3 – 4.5) at this pH (Agogbua and Wynn 1976).

2.2. *In vitro release*

The release of the enzymes from the nanoparticles was assessed *in vitro* in purified water (MilliQ), TRIS buffer (pH 7.4), and human blood plasma (Fig. 5). Since phosphate is a competitive inhibitor of arylsulfatases (Baum et al. 1959), TRIS buffer was used in this study instead of usually used phosphate buffer saline (PBS). The nanoparticulate formulation of ASA is intended for the intravenous administration; at the same time it is known that in the bloodstream the particles quickly can adsorb to plasma proteins (Moghimi et al. 2001; Lundqvist et al. 2011) which in turn may cause displacement of ASA from their surface. Indeed, while the release rates of ASA and ASB in water were constant over the time (ASA about 21.1%, ASB 5.4%), in TRIS buffer and blood plasma ASA showed a burst release of 19 % and of 53 %, respectively, compared to water as the release medium. After 60 min incubation ASA desorption increased to the extent of 70 % in TRIS and 90 % in plasma.

Desorption of ASB from the particles was similar in TRIS and in human blood plasma and reached 35 % and 38 %, respectively, compared to water after 60 min incubation. In both cases, considerable desorption took place immediately after dilution (the so called "burst-effect") again being indicative of Langmuir kinetics. Thus the burst release of ASB in plasma amounted to 28 %. The more considerable burst release of ASA that reached 71 %, might be due to ASA dimerisation leading to a less effective interaction of this enzyme with the particle surface. At neutral pH, dimers dissociate and ASA is released faster than ASB. In addition, ASA has a higher negative charge at the plasma pH (7.4), due to the lower pI (Table 1), which may also contribute to a more prominent desorption of this enzyme.

Nevertheless, based on the results of the previous experiments, these data suggest that the stability of the formulation in blood plasma may be sufficient for a delivery of the arylsulfatases to the brain. The transport of polysorbate 80-coated nanoparticles across the BBB is a very rapid process. Zensi et al. (2009) found nanoparticles in the brain endothelial cells of mice and rats already 15 min after intravenous injection, and pronounced pharmacological effects (nociception) with dalargin (Kreuter et al. 1997) or loperamide (Alyautdin et al. 1997) bound to the PBCA nanoparticles.were achieved after the same time.

2.3. *Freeze-drying*

In addition, freeze-drying experiments with arylsulfatase A as well as B were performed as this is a very usefull method for the long term storage and conservation of proteins (Abdelwahed et al. 2006; Carpenter et al. 1997; Fischer et al. 2008; Jiang and Nail 1998). This experiment was performed in order to investigate the stability of ASA and ASB free or bound to the nanoparticles after freeze-drying in the presence of various lyoprotective excipients.

Samples of ASA and ASB as well as their nanoparticulate formulations were freeze-dried, stored at 21 °C, and redispersed after a period of at least 8 weeks. The level of the ASB activity was measured after 8 weeks. The activity of ASA was measured immediately after freeze-drying as well as after 2, 6, and 8 weeks of storage at 21 °C. Redispersed enzyme solutions and nanoparticle suspensions were analysed by pNCS activity assay as well as SEC. As detected with pNCS, freeze-drying of ASB in solution led to a 73.7 ± 0.9 % loss of activity, whereas the activity of ASB adsorbed to the nanoparticles decreased only by 43.8 ± 6.3 % in the absence of any lyoprotective agent. The best activity results for ASB were obtained with addition of lactose and sucrose (Fig. 6).

Since the lactose and proteins tend to form adducts (Maillard reaction) (Anhorn et al. 2008; Fischer et al. 2008), sucrose was used for further experiments with ASA. Fig. 6 shows the feasibility of preserving the activity of ASB after freeze-drying in the presence of 3% of sucrose. No dimerisation or aggregation of enzyme could be detected by SEC (data not shown).

In a second step, ASA free or bound to the nanoparticles were freeze-dried using sucrose as a lyoprotectant in a concentration of 3%. As shown in Fig. 7, after 8 weeks of storage, the pure enzyme retained about 90% of activity. Even better results were detected for ASA adsorbed onto PBCA nanoparticles: in this case no loss of activity could be detected.

2.4. *Conclusions*

This study demonstrates the feasibility of arylsulfatase A adsorption onto PBCA nanoparticles. The maximum capacity was 59 μg of enzyme per 1 mg of PBCA. The ASA-loaded PBCA nanoparticles are a stable formulation which can be easily freeze-dried and stored over a period of at least 8 weeks. The known ability of this carrier to deliver drugs to the brain suggests that the PBCA-based formulation of ASA is a potential candidate for the enzyme replacement therapy of metachromatic leukodystrophy.

3. Experimental

3.1. *Chemicals*

Arylsulfatase B (N-acetylgalactosamine-4-sulfate sulfatase, Naglazyme® 1 mg/ml) was obtained from BioMarin Europe Ltd., Novato, CA, USA; arylsulfatase A (rhASA 4.2 mg/ml) was obtained from Shire plc., St Helier, UK; *n*-butyl-2-cyanoacrylate (Sicomet®) from Sichel-Werke, Hannover, Germany; 0.1 N hydrochloric acid and 1 N sodium hydroxide from VWR, Darmstadt, Germany; dextran 70'000, p-nitrocatechol sulphate (pNCS), and human serum albumin (HSA) from Sigma, St. Louis, MO, USA; hydroxymethylaminomethane (TRIS) from Molekula, Gillingham, UK; mannitol, lactose monohydrate, sucrose, and trehalose from Merck KGaA, Darmstadt, Germany. Other chemicals were of analytical grade.

3.2. *Nanoparticle preparation*

The PBCA nanoparticles were prepared by anionic polymerisation, as described previously (Mühlstein et al. 2013; Couvreur et al. 1979): 1 % of *n*-butyl-2-cyanoacrylate was added to a 1 % dextran 70000 solution in 0.01 N hydrochloric acid with constant stirring. Stirring was continued for 2.5 h, subsequently the polymerisation was completed by neutralisation with 0.1 N sodium hydroxide. The mixture was filtered through a G2 sintered glass filter (Schott, Mainz, Germany) with a pore size of 40 – 100 μm to remove agglomerates and then lyophilised with 3 % mannitol as a lyoprotector or used as suspension.

3.3. *Determination of particle yield*

The particle content was determined by gas chromatography (GC), as described by Langer et al. (1994). For this purpose, PBCA nanoparticles were hydrolysed for 12 h with 2 N sodium hydroxide solution, and free n-butanol formed upon hydrolysis was extracted with dichloromethane. Sample (1 μl) was injected into the GC system (Hewlett-Packard 5890 Series II; Hewlett-Packard, Wilmington, United States), and the concentration of *n*-butanol was measured using pentanol as internal standard. The particle yield was calculated as mg of n-butyl-cyanoacrylate per ml suspension.

3.4. *Adsorption of ASA to the PBCA nanoparticle surface*

In order to determine the ASA adsorption to the PBCA nanoparticles, the freeze-dried particles were resuspended in aqueous solutions of ASA and incubated at 4 °C under constant stirring (650 rpm, Thermomix, Germany) for 1 h. The concentration of ASA was always 2.5 mg/ml, pH values ranged from 4.5 to 7.3. After incubation samples were analysed as described below.

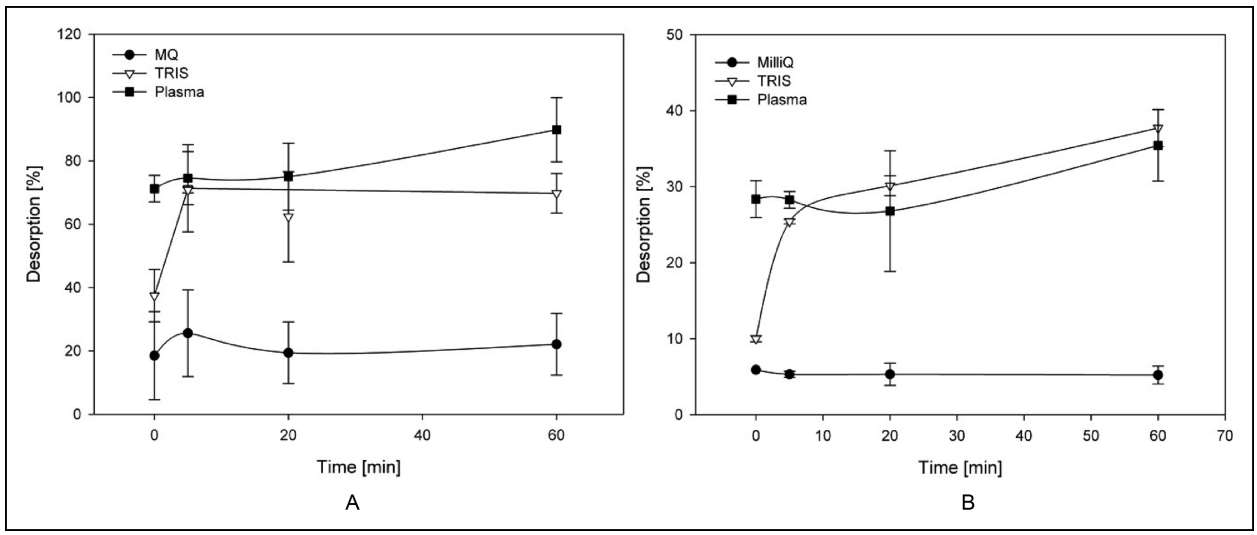

Fig. 5: Relative drug desorption [%] of ASA (A) and ASB (B) in different desorption media (TRIS buffer pH 7.4 and human plasma) compared to water (n = 3; mean ± S.D.).

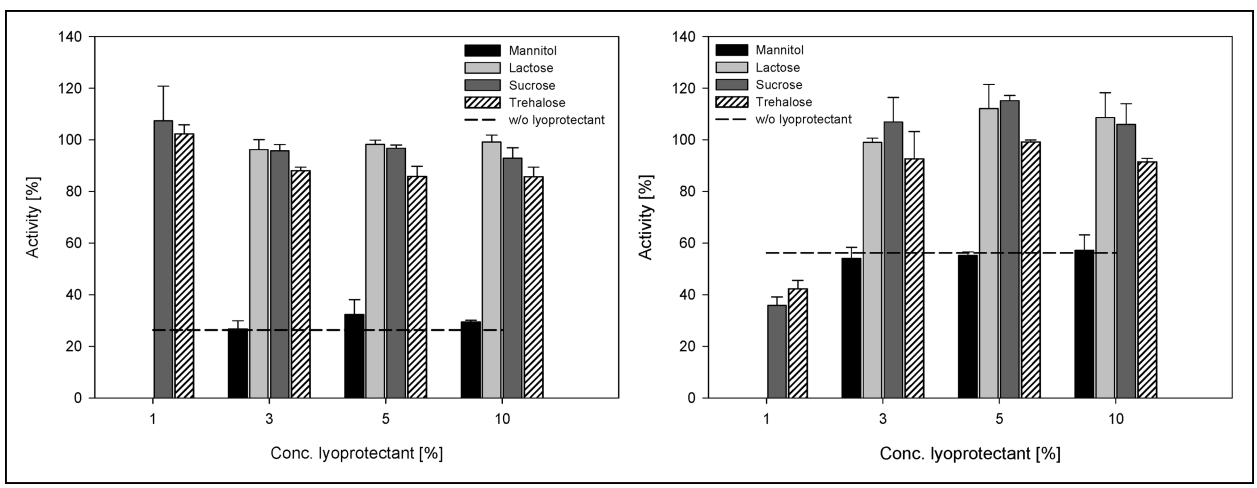

Fig. 6: Activity of ASB (A) and ASB bound to PBCA nanoparticles (B) 8 weeks after freeze-drying using different lyoprotectants in various concentrations (n = 3; mean ± S.D.).

3.5. Determination of ASA binding to PBCA nanoparticles

Efficacy of ASA binding to the nanoparticles was determined indirectly by measurement of the amount of free ASA in the supernatant after separation of the nanoparticles by centrifugation (20000 g; 30 min) (Eq. (2)). The measurements were performed by size exclusion chromatography (SEC) and enzyme activity assay in order to determine changes in enzyme conformation and loss of activity.

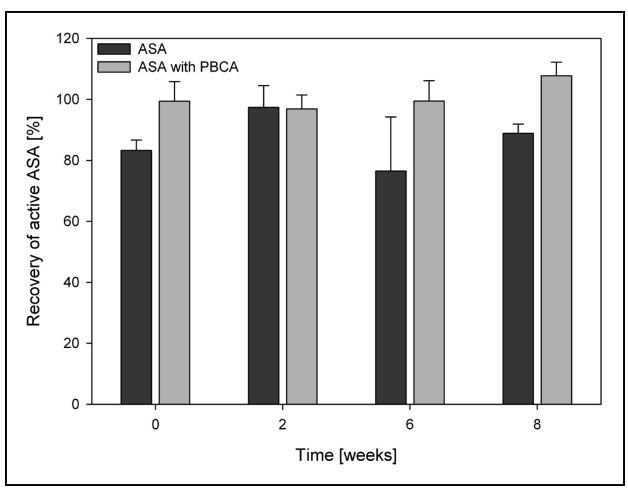

Fig. 7: Activity of ASA and ASA bound to PBCA nanoparticles after freeze-drying compared to freshly prepared ASA preparations after various storage times (n = 3; mean ± S.D.).

3.5.1. Enzyme activity assay

The activity assay of ASA and ASB was performed as described earlier (Baum et al. 1959), using *p*-nitrocatechol sulphate (pNCS) as a substrate. A 10 mM pNCS solution was added to the diluted samples and incubated for 30 min at 37 °C under constant shaking (650 rpm, Thermomix, Germany). The reaction was terminated by addition of 200 µl of a 1 N sodium hydroxide solution. The absorption of the resulting 4-nitroquinone was measured at 515 nm ($\varepsilon = 12.400\ M^{-1}cm^{-1}$ (Baum et al. 1959), U-3000 spectrometer, Hitachi Ltd., Tokyo, Japan).

3.5.2. Measurement of ASA/ASB concentration by size exclusion chromatography (SEC)

The amount of free enzyme was measured using a SEC system (Merck Hitachi) equipped with a Shodex Protein 800 KW column (Showa Denko K.K., Tokyo, Japan). Phosphate buffer (pH 6.6) was used as eluent. The ASA was detected by spectrophotometry at 280 nm and the content was calculated using a calibration curve of ASA in known concentrations.
The amount of adsorbed ASA was calculated using the following equation (Eq. (2)):

$$Drug \rightleftarrows loading[\%] = \frac{m(totaldrug) - m(freedrug)}{m(totaldrug)} \cdot 100 \qquad (2)$$

3.6. Measurements of particle size and zeta-potential

The resulting nanoparticles were characterised by photon correlation spectroscopy (PCS) and zeta-potential using a Nanosizer ZS (Malvern Instruments Ltd., Malvern, UK): the mean diameter and polydispersity were measured by PCS, zeta-potential was assessed using Laser-Doppler micro-electrophoresis in a palladium electrode dip cell (Malvern). For size measurements the samples were diluted 1:50 with purified water; the scat-

tering angle was 173°; the temperature was set to 25 °C. The zeta-potential was measured using the non-diluted samples.

3.7. *In vitro release kinetics*

The ASA-loaded nanoparticles in suspension were diluted 10-fold with either MilliQ water, or TRIS buffer (pH 7.4), or human blood plasma. The samples were analysed immediately after dilution and after 5, 20, and 60 min. The released enzyme was separated from the nanoparticles by centrifugation (30 min, 20000 g). The obtained supernatant was analysed using the activity assay described above. Using the following equation (Eq. (3)) the percentage of release was calculated:

$$release[\%] = \frac{c_{ads} - c_t}{c_{ads}} \cdot 100 \quad (3)$$

where: c_{ads}, concentration of ASA previously adsorbed [μg/ml], c_t, concentration of ASA in the eluent at the time [μg/ml],

3.8. *Freeze-drying*

After adsorption of ASA to the nanoparticles, 50 to 500 μl of a 20% (w/v) solution of mannitol, lactose, sucrose, or trehalose were added to 500 μl of the suspension. Subsequently the suspension was diluted to 1 ml with purified water (MilliQ) (Millipore Merck KGaA, Darmstadt, Germany). In total, the samples contained 0.25 μg enzyme, 1.65 μg PBCA nanoparticles, and 1%, 3%, 5%, or 10% of lyoprotective agent. The samples containing free enzyme without nanoparticles were prepared likewise by taking 500 μl of enzyme solution and appropriate amount of a lyoprotective agent. The samples of ASA without any addition of excipients were used as controls. Freeze-drying was performed using a Christ Epsilon 1–4 freeze-dryer (Martin Christ GmbH, Osterode, Germany). Samples were frozen for 3.5 h at −60 °C before the primary drying process was started. Then the shelf temperature was increased over 1 h up to −35 °C, and the pressure was reduced to 0.94 mbar. Subsequently, the temperature was increased to -10 °C at a pressure of 0.006 mbar. After 37 h of primary drying, the secondary phase started by increasing the temperature up to 10 °C within 1 h. Then the temperature was increased to the final temperature of 20 °C and 0.006 mbar was hold for further 10 h. At the end of the process, freeze-drying vials were plugged and stored at 21 °C. After resuspension in 1 ml of MilliQ water and ultrasonication (3 min, Sonorex, Bandelin electronic GmbH, Berlin, Germany), the amount of active enzyme was determined by pNCS method and compared to that of freshly prepared samples. A SEC analysis was performed using freeze-dried ASA solution in order to detect any possible aggregation.

3.9. *Statistical analysis*

The statistical analysis of samples was performed using the Student's t-test; the differences were considered to be statistically significant for $p < 0.05$. All data reported are mean values ± standard deviations.

Acknowledgements: This study was supported by a grant of the Brains for Brain (B4B) Foundation, Padova, Italy. The authors also would like to thank Prof. M. Beck from the Children's hospital, Gutenberg University Mainz, Germany for a generous gift of arylsulfatase B.

References

Abdelwahed W, Degobert G, Stainmesse S, Fessi H (2006) Freeze-drying of nanoparticles: formulation, process and storage considerations. Adv Drug Deliv Rev 58: 1688–1713.

Agogbua SI, Wynn CH (1976) Purification and properties of arylsulphatase B of human liver. Biochem J 153: 415–421.

Alyautdin RN, Petrov VE, Langer K, Berthold A, Kharkevich DA, Kreuter J (1997) Delivery of loperamide across the blood-brain barrier with polysorbate 80-coated polybutylcyanoacrylate nanoparticles. Pharm Res 14: 325–328.

Alyautdin RN, Tezikov EB, Ramge P, Kharkevich DA, Begley DJ, Kreuter J (1998) Significant entry of tubocurarine into the brain of rats by adsorption to polysorbate 80-coated polybutylcyanoacrylate nanoparticles: an in situ brain perfusion study. J Microencapsul 15: 67–74.

Anhorn MG, Mahler HC, Langer K (2008) Freeze-drying of human serum albumin (HSA) nanoparticles with different excipients. Int J Pharm 363: 162–169.

Baum H, Dodgson KS, Spencer B (1959) The assay of arylsulphatases A and B in human urine. Clin Chim Acta 4: 453–455.

Beck M (2007) New therapeutic options for lysosomal storage disorders: enzyme replacement, small molecules and gene therapy. Hum Genet 121: 1–22.

Beck M (2010) Therapy for lysosomal storage disorders. IUBMB Life 62: 33–40.

Bond CS, Clements PR, Ashby SJ, Collyer CA, Harrop SJ, Hopwood JJ, Guss JM (1997) Structure of a human lysosomal sulfatase. Structure 5: 277–289.

Carpenter JF, Pikal MJ, Chang BS, Randolph TW (1997) Rational design of stable lyophilized protein formulations: some practical advice. Pharm Res 14: 969–975.

Cha P, Krishnan A, Fiore VF, Vogler EA (2008) Interfacial energetics of protein adsorption from aqueous buffer to surfaces with varying hydrophilicity. Langmuir 24: 2553–2563.

Couvreur P, Kante B, Roland M, Guiot P, Bauduin P, Speiser P (1979) Polycyanoacrylate nanocapsules as potential lysosomotropic carriers: preparation, morphological and sorptive properties. J Pharm Pharmacol 31: 331–332.

Dali, C. and Lund, A.M. (2009) Intravenous enzyme replacement therapy for metachromatic leukodystrophy (MLD). Abstract from the Annual Clinical Genetics (ACMG) Meeting on 25 March 2009 in Tampa, FL. Available at: http://mldfoundation.org/pdfs/Shire-ERT-P12-2009-02.pdf.

Fischer S, Hoernschemeyer J, Mahler HC (2008) Glycation during storage and administration of monoclonal antibody formulations. Eur J Pharm Biopharm 70: 42–50.

Ghosh D (2007) Human sulfatases: a structural perspective to catalysis. Cell Mol Life Sci 64: 2013–2022.

Gibson GJ, Saccone GT, Brooks DA, Clements PR, Hopwood JJ (1987) Human N-acetylgalactosamine-4-sulphate sulphatase. Purification, monoclonal antibody production and native and subunit Mr values. Biochem J 248: 755–764.

Gieselmann V (1995) Lysosomal storage diseases. Biochim Biophys Acta 1270: 103–136.

Gieselmann V, Krageloh-Mann I (2010) Metachromatic leukodystrophy – an update. Neuropediatrics 41: 1–6.

Heim P, Claussen M, Hoffmann B, Conzelmann E, Gartner J, Harzer K, Hunneman DH, Kohler W, Kurlemann G, Kohlschutter A (1997) Leukodystrophy incidence in Germany. Am J Med Genet 71: 475–478.

Jiang S, Nail SL (1998) Effect of process conditions on recovery of protein activity after freezing and freeze-drying. Eur J Pharm Biopharm 45: 249–257.

Koutsopoulos S, Patzsch K, Bosker WT, Norde W (2007) Adsorption of trypsin on hydrophilic and hydrophobic surfaces. Langmuir 23: 2000–2006.

Kolodny EH. 1989. Metachromatic leukodystrophy and multiple sulfatase deficiency: Sulfatide lipidosis. In: Scriver CR, Beaudet AL, Sly WS, Valle DE, eds. The metabolic basis of inherited disease. New York: p.1721–50.

Kreuter J, Petrov VE, Kharkevich DA, Alyautdin RN (1997) Influence of the type of surfactant on the analgesic effects induced by the peptide dalargin after its delivery across the blood–brain barrier using surfactant-coated nanoparticles. J Control Release 49: 81–87.

Kreuter J (2001) Nanoparticulate systems for brain delivery of drugs. Adv Drug Deliv Rev 47: 65–81.

Krishnan A, Liu YH, Cha P, Allara D, Vogler EA (2006) Interfacial energetics of globular-blood protein adsorption to a hydrophobic interface from aqueous-buffer solution. J R Soc Interface 3: 283–301.

Kufleitner J, Wagner S, Worek F, von Briesen H, Kreuter J (2010) Adsorption of obidoxime onto human serum albumin nanoparticles: drug loading, particle size and drug release. J Microencapsul 27: 506–513.

Kurakhmaeva KB, Djindjikhashvili IA, Petrov VE, Balabanyan VU, Voronina TA, Trofimov SS, Kreuter J, Gelperina S, Begley D, Alyautdin RN (2009) Brain targeting of nerve growth factor using poly(butyl cyanoacrylate) nanoparticles. J Drug Target 17: 564–574.

Langer K, Seegmüller E, Zimmer A, Kreuter J (1994) Characterisation of polybutylcyanoarylate nanoparticles: I. Quantification of PCBA polymer and dextrans. Int J Pharm110: 21–27.

Lukatela G, Krauss N, Theis K, Selmer T, Gieselmann V, von Figura K, Saenger W (1998) Crystal structure of human arylsulfatase A: the aldehyde function and the metal ion at the active site suggest a novel mechanism for sulfate ester hydrolysis. Biochemistry 37: 3654–3664.

Lundqvist M, Stigler J, Cedervall T, Berggard T, Flanagan MB, Lynch I, Elia G, Dawson K (2011) The evolution of the protein corona around nanoparticles: a test study. ACS Nano 5: 7503–7509.

McGonigle P (2012) Peptide therapeutics for CNS indications. Biochem Pharmacol 83: 559–566.

Moghimi SM, Hunter AC, Murray JC (2001) Long-circulating and target-specific nanoparticles: theory to practice. Pharmacol Rev 53: 283–318.

Mollmann SH, Jorgensen L, Bukrinsky JT, Elofsson U, Norde W, Frokjaer S (2006) Interfacial adsorption of insulin conformational changes and reversibility of adsorption. Eur J Pharm Sci 27: 194–204.

Mühlstein A, Gelperina S, Kreuter J (2013) Development of nanoparticle-bound arylsulfatase B for enzyme replacement therapy of mucopolysaccharidosis VI. Pharmazie, 68: 549–554.

Pardridge WM (2005) Molecular biology of the blood-brain barrier. Mol Biotechnol 30: 57–70.

Pardridge WM (2007a) Blood-brain barrier delivery. Drug Discov Today 12: 54–61.

Pardridge WM (2007b) Blood-brain barrier delivery of protein and non-viral gene therapeutics with molecular Trojan horses. J Control Release 122: 345–348.

Poorthuis BJ, Wevers RA, Kleijer WJ, Groener JE, de Jong JG, van Weely S, Niezen-Koning KE, van Diggelen OP (1999) The frequency of lysosomal storage diseases in The Netherlands. Hum Genet 105: 151–156.

Rubin LL, Staddon JM (1999) The cell biology of the blood-brain barrier. Annu Rev Neurosci 22: 11–28.

Scheld WM (1989) Drug delivery to the central nervous system: general principles and relevance to therapy for infections of the central nervous system. Rev Infect Dis 11 Suppl 7: S1669–1690.

Sommerlade HJ, Selmer T, Ingendoh A, Gieselmann V, von Figura K, Neifer K, Schmidt B (1994) Glycosylation and phosphorylation of arylsulfatase A. J Biol Chem 269: 20977–20981.

Soppimath KS, Aminabhavi TM, Kulkarni AR, Rudzinski WE (2001) Biodegradable polymeric nanoparticles as drug delivery devices. J Control Release 70: 1–20.

von Figura K, Gieselmann V, Jaeken J. 2001. Metachromatic Leukodystrophy. In: Scriver C, Beaudet A, Sly W, Valle D, Childs B, Kinzler K, Vogelstein B, eds. The Metabolic and Molecular Bases of Inherited Disease. New York: p. 3695–3724.

Wohlfart S, Gelperina S, Kreuter J (2012) Transport of drugs across the blood-brain barrier by nanoparticles. J Control Release 161: 264–273.

Yaghootfam A, Schestag F, Dierks T, Gieselmann V (2003) Recognition of arylsulfatase A and B by the UDP-N-acetylglucosamine: lysosomal enzyme N-acetylglucosamine-phosphotransferase. J Biol Chem 278: 32653–32661.

Zensi A, Begley D, Pontikis C, Legros C, Mihoreanu L, Wagner S, Buchel C, von Briesen H, Kreuter J (2009) Albumin nanoparticles targeted with Apo E enter the CNS by transcytosis and are delivered to neurones. J Control Release137: 78–86.